EDGE Oriented Image Denoising Through an Adaptive Thresholding in the Complex Wavelet Domain

B.ChinnaRao, M.Madhavilatha

Abstract: ***Noise reduction is a fundamental process in the enhancement of image quality. In recent years, large bodies of approaches have been developed to minimize the effect of noise in the image based applications. In this study, the authors proposed a novel image denoising framework based on applying adaptive thresholding on complex wavelet transform methods. In the proposed approach, the adaptive thresholding has high capacity to tune its parameters according to the noise type and noise intensity. Further, focusing over the preservation of edges with minimum complexity, this paper proposed a new patch grouping mechanism based on the Gabor wavelet coefficients. Simulation experiments are employed over the image samples to evaluate the performance of proposed mechanism by quantifying the signal strength, structural preservation and edge preservation with respect to the PSNR, SSIM and FOM. In the experiments, the proposed approach had shown an optimal performance in both the edge preservation and quality enhancement with less computational burden.***

Keywords: ***Image Denoising, DT-CWT, Gabor Filter, Bayesian Shrink, PSNR, SSIM, FOM.***

I. INTRODUCTION

Image processing plays an important role in various fields including, medical imaging, artificial intelligence, security surveillance, facial recognition, and robotic vision [1-4]. Mainly processing an image is these fields mainly depend on the quality of image. The overall performance of image processing applications is completely dependent on the quality of test image. For example, in the case of face recognition system, the recognition framework detects the facial image based on the facial images and the recognition accuracy will be more only if the test facial imagery is more qualitative. However, the images are inevitably composed of noise during acquisition and transmission. Due to the uneven environments during the image acquisition, the captured consists of external noises also. Furthermore, due to different lighting conditions, the acquitted image consists of blur along with noise. Image denoising aims to reconstruct an image from its noise corrupted version and tends to enhance the degraded image quality for better analysis in different image oriented applications. Hence, image denoising is a fundamental aspect and an important procedure for many image processing systems [5].

Depends on the methodology and domain accomplished image for denoising, the earlier approaches are categorized as spatial domain approaches and transform domain approaches. Spatial domain approaches are further classified as non-linear filters [6] and linear filters [7]. The spatial filters generally accomplish low-pass filtering over the image to remove the noise. However, the spatial filters eliminate the noise to a reasonable extent but at the cost of blurring the image such that the edges and textures become invisible. The transform domain filters initially transforms the image and then different methodologies are accomplished over the transformed coefficients to remove the noise. Based on the methodology, the transform domain approaches are further classified as wavelet domain approaches and other spatial frequency approaches [15].

In the wavelet based methods, initially the image is decomposed into sub bands through wavelet filters and then some thresholding is applied to remove the noise content from wavelet coefficients. Based on this, the wavelet domain approaches are further classified as Linear Filtering [8,9], Non-linear threshold filtering [10], wavelet coefficient model [13, 14] and non-orthogonal wavelet transform [11, 12]. Linear filtering methods accomplished wiener filter to remove the noise through mean square error (MSE). In the case of non-linear thresholding, a threshold is defined considering the overall characteristics of all coefficients and then the noise is removed by comparing every coefficient with predefined threshold. Examples of such thresholding are SUREShrink [16], MultiShrink [17], BayesShrink [18], BiShrink [19], ProbSHrink [20], and VisuShrink [21].However, all these threshold schemes will cut off parts of the signals and leaves some noise untouched.

Though a vast research was accomplished over image denoising, still there is a room to improve the quality of image by denoising it properly. Among all those approaches, some are focused on the quality and some are focused on the complexity. The complexity arises due to the consideration of all pixels instead of their characteristic. However, no method is proposed in earlier considering providing a tradeoff between the complexity and quality. If quality was focused, the complexity needs to compromise and vice versa. Hence to overcome this problem, this paper proposes a new image denoising framework in the transform domain through Dual tree complex wavelet Transform (DT-CWT). Further, the preservation edge pixels are also important in the denoising process, this paper also proposed a novel grouping mechanism to cluster the pixels with similar properties into a single group. Further an adaptive threshold is derived in this paper. Extensive simulation is carried out over different gray scale images at different noise levels and at different noise types and the performance

Revised Manuscript Received on December 22, 2018.

B.ChinnaRao, Associate Professor, Department of ECE, MLR Institute of Technology, Hyderabad, Telangana, India.

Dr.M.Madhavilatha, Professor, Department of ECE, JNTU College of Engineering, Hyderabad, Telangana, India.

is measured with the performance metrics such as PSNR and SSIM for varying noise levels.

Reminder of the paper is organized as follows; Section II illustrates the details of literature survey, section III describes the complete details of proposed approach. Simulation results are discussed in section IV and finally conclusions are provided in section V.

II. LITERATURE SURVEY

In earlier, so many approaches are developed to filter out noise from image. As per above discussion, the transform domain approaches are better compared to the spatial domain approaches. Moreover, the wavelet based methods are effective in the transform domain approaches. Here the literature is carried out only on the earlier developed image denoising approaches based on wavelet transform.

An optimal wavelet packet thresholding based image denoising framework was proposed by A. Fathi and A. R. Naghsh-Nilchi [22] based on the Generalized Gaussian Distribution (GTD). Using Shannon entropy, this approach decomposes noise image into best tree and selects an adaptive threshold value depending on the statistical parameters of subband. Next, the transformed coefficients obtained through multi-level wavelet decomposition are processed through the singular value decomposition (SVD) and a patch based weighted SVD filtering technique is proposed by P.Jain and V.Tyagi [23] to preserve the important features while filtering out the noise from a noisy image. Further, a new method was proposed by Wang et.al, [24] by combining the wavelet transform with SVD, with enhancement of the directional filters. First, the noisy image was decomposed into low frequency and high frequency sub bands through wavelet transform, with the extracted edges and retained to avoid the loss of information at edges. In order to improve the denoising effect of the conventional approaches, a new thresholding function is proposed by He et.al, [25] by considering the interscale correlation. Firstly a new correlation index [27] is proposed based on the propagation characteristics of wavelet coefficients and then a threshold determining mechanism is discovered based on the correlation index. In [26], a novel Bayesian multiscale approach is proposed to remove the speckle noise form Synthetic Aperture Radar (SAR) images through a non-homomorphic framework. Since the speckle noise is multiplicative in nature, a linear decomposition was used to realize this. Further, to capture the noise free reflectivity in the heavy-tailed stationary wavelet coefficients, a two-sided GTD is introduced in the SWT domain.

A homomorphic method was proposed by Singh and Shree [28-30] using noise thresholding method where anisotropic diffusion is applied as a pre-processing for 2D-DWT. Wiener and median filters are used over the approximation band of image to remove the blurring. Further the noise thresholding method is applied as the post-processing step in the despeckling process. Though this method achieved better results in the elimination of speckle noise and edge preservation, but still there is a scope to improve by the intelligent use of noise method. Manoj Diwakar and kumar proposed a new noise filtering method based on wiener filtering and wavelet packet thresholding algorithm [31]. This approach eliminates the noise more effectively and also removes the blur but some high contrast and high textured areas are unprocessed.

Manoj Diwakar [32] proposed a two-step image denoising scheme to remove the noise in CT images. First, this method accomplished wavelet thresholding followed by a noise thresholding mechanism. In the second step, this work focused on the aggregation in the wavelet domain. Sethunadh R and Thomas T [33] developed a new and adaptive SAR image despeckling framework based on the directionalet transform and also the property of statistical interscale dependency. This approach achieved better results in the preservation of textures regions in SAR images. Considering the advantages of DT-CWT, Ranjani et.al, [34] presented a SAR image despeckling based on the interscale dependency. This method accomplished maximum a posterior in the proposed framework and achieved a better results in the removal of speckle noise from satellite images. Bin Xu et.al, [35] presented an image denoising method to filter out the speckle noise based on patch order and transform domain filtering. Bias corrected Log Transform is implemented on SAR image to realize the multiplicative nature of speckle noise.

All the above methods are focused on the quality preservation only. But, most of the approaches not focused over the complexity. The complexity is an important factor which needs to be considered during image denoising. However, almost all the above mentioned approaches tried to consider every coefficient in the denoising process. This process constitutes a computational burden over the denoising system. Hence some methods tried to overcome this issue by developing a grouping technique through which the coefficients/pixels with similar properties into a single group [39-43]. A most advantageous approach focused towards this achievement is proposed by Dabov et.al, [36],Block-Matching and 3-D (BM3D) filtering and Maggioni et.al, [37], BM4D filtering. Recently, B. C. Rao [38] proposed a new patch grouping mechanism with an aim of preservation of edges features during the denoised process with less complexity. This approach proposed a new thresholding mechanism along with patch grouping based on the spectral features of wavelet coefficients.

III. PROPOSED APPROACH

The complete accomplishment of proposed approach is done in five phases namely, Decomposition through DT-CWT, Patch Grouping based on the Gabor filter oriented edges, Thresholding, fusion and inverse DT-CWT. In the first phase, the noisy image is decomposed through DT-CWT into approximation and detailed sub bands. Further to preserve the edge information, this paper accomplished Gabor filter oriented edge features evaluation in the high frequency bands. Next, based on the Gabor Edges features, the overall sub bands are clustered into some groups based in the similarity in the properties. Once the patches are grouped into patches, they are processed for thresholding. Here the thresholding is accomplished in two phase, one is through Bayesian Shrinkage rule and another is through

adaptive thresholding based on the energies of wavelet coefficients. Next, a fusion mechanism is accomplished over the denoised patches based on the correlation and finally the denoised patches are processed for reconstruction through inverse DT-CWT. The overall block diagram of proposed denoising approach is depicted in figure.1.

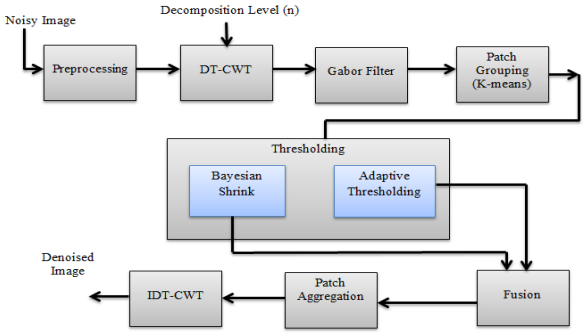

Figure.1 Overall Block Diagram of Proposed mechanism

A. Entropy Evaluation

In the image denoising methods, most of the wavelet based denoising approaches didn't given a perfect idea about the decomposition levels. In the process of noise removal, initially the noisy image is decomposed through wavelet transform into some sub bands. However, there is no detailed information about the decomposition levels, i.e., up to how many levels, the noisy image has to decompose? No method is developed in earlier based on the level of decomposition. Since the level of decomposition is also an important aspect in the image analysis, it is also need to be considered. As the number of levels increases, the number of bands also increases by which the denoising system has to bear an extra computational burden. On the other hand, if the number of bands is very less, the image can't be analyzed more effectively due to the limited information reveal about the characteristics of image. Hence, there is a need to define the number of levels. Moreover, the process of finding the sufficient decomposition level must be robust for all types of image and also for all types of noise. To this extent, a novel mechanism is proposed in this paper to define the decomposition level.

This mechanism is based on the texture measurement using entropy parameter for better results [29]. Here the entropy parameter is accomplished to measure the uncertainty in the texture of the wavelet coefficients at every decomposition. Once the image was decomposed into Low frequency and high frequency sub bands through wavelet transform, the entropy is measured for both image and the obtained bands. For example, *I* be an image and *LL1*, *LH1*, *HL1* and *HH1* are the obtained sub bands obtained after the n^{th} level decomposition of I, then the entropies of both image and sub bands are denoted as E_I, E_{LL}, E_{LH}, E_{HL}, and E_{HH}. If the average entropy of sub bands such as E_{LL}, E_{LH}, E_{HL}, and E_{HH} are observed to be greater than the entropy of image, E_I, then the decomposition process will stop and the level *n* is declared as an optimal decomposition level. In the case of E_I greater than the average of E_{LL}, E_{LH}, E_{HL}, and E_{HH}, then the decomposition will proceed to further level. The entropy is formulated as,

$$E = -\sum_i p_i \log_2 p_i \quad (1)$$

B. Gabor Filter Oriented Edges

The two dimensional (2D) Gabor Filter decomposes an image into components of different orientations and scales [44]. This filter helps in the capturing of the visual characteristics of image such as orientation selectivity, spatial localization, and spatial frequency. The 2D Gabor filter is a complex exponential cantered at a given frequency and modulated by Gaussian Envelope. Due to the presence of complex exponential, the obtained results consist of both real and imaginary parts. To determine the orientation features of an image, the Gabor filter can be accomplished. The general form of real part is formulated as;

$$G(x,y,\sigma_x,\sigma_y,f,\theta) = exp\left[-\frac{1}{2}\left(\left(\frac{x'}{\sigma_x}\right)^2+\left(\frac{y'}{\sigma_y}\right)^2\right)\right] \quad (2)$$

Where

$$x' = x\cos(\theta) + y\sin(\theta) \quad (3)$$
$$y' = y\cos(\theta) - x\sin(\theta) \quad (4)$$

And

σ_x and σ_y are the standard deviations of Gaussian Envelope along the x-axis and y-axis respectively. The parameters, θ and f are the rotation angle and central frequency of Gabor filters respectively. To obtain a Gabor filtered output, $GF(x, y)$ of an image $I(x, y)$, it needs to be convolved with Gabor filter as specified in eq.(2), like

$$GF(x,y) = G(x,y,\sigma_x,\sigma_y,f,\theta) * I(x,y) \quad (5)$$

Next, the Gabor filtered output is processed for further accomplishment. In this paper, the Gabor filter is used as directional filter to find out the possible orientation in which the image features re dominating and to find the difference between the image pixels those are noisy and noise free. To perfectly discriminate the difference between the edge pixels and smooth pixels, the Gabor filter is a better option. Since the accomplishment of a Gabor filter over an image of a sub band resolves the confusion about the edge pixels and noisy pixels through the Orientational analysis, it is very helpful in this aspect. A simple representation of the Gabor filter outputs at different rotation angles is represented in figure.1

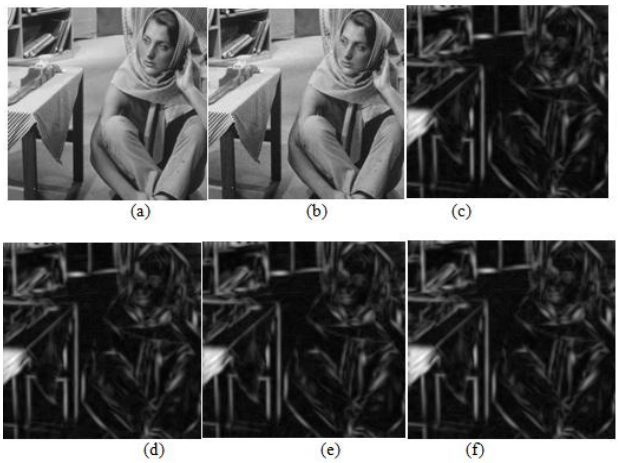

Figure.2 Results of Gabor Filter over a Noisy image, (a) Original Image, (b) Noisy image, Gabor filtered image at (c) θ=00, (d) θ=450, (e) θ=900, and (f) θ=1350.

The Gabor filter can be realized as direction al filter through which the edge pixels dominant orientation can be extracted such that the pixels with edges ad pixels with noise are discriminated more perfectly. After obtaining the Gabor filter outputs, the Gradients are measured to find out the Gradient similarity in all orientations. Based on the Gradient similarity, the complete pixels of image are grouped into some clusters. The gradient similarity is evaluated according to the methodology specified in [45]. In [45], the gradient similarity is found between the successive pixels to find the similarity of pixels and used the obtained similarity in the patch grouping. Furthermore, the method described in the [45] accomplished K-means clustering algorithm to cluster the coefficients with similar properties into a same cluster. The same methodology is accomplished in this paper to perform patch grouping and once all the coefficients are grouped into the patches, an adaptive thresholding is applied over the patches to filter out the noise.

C. Thresholding

Once the patches are obtained, this approach accomplishes an adaptive thresholding over the patches. In this paper, two different threshold mechanisms are proposed to perform thresholding. Further the obtained outputs at both mechanisms are fused through fusion rule. The first thresholding method considered here is wavelet thresholding using Bayesian Shrinkage rule and another is an adaptive thresholding proposed in [45]. The details of adaptive wavelet thresholding concept is completely described in the reference [45] and for simple idea the wavelet thresholding using Bayesian shrinkage rule is formulated as follows [26];

According to this rule, the threshold λ is defined as

$$\lambda = \frac{\sigma_n^2}{\sigma_Y} \quad (6)$$

Where σ_n^2 is the noise variance and it is measured as

$$\sigma_n^2 = \left[\frac{Median(|X(x,y)|)}{0.6745} \right] \quad (7)$$

Where $X(x, y) \in LH, HL, HH$. The standard reference Bayesian shrinkage method is applied only over the HH band but this paper applied over all the detailed bands. Further the σ_Y is standard deviation of image Y and it is measured as

$$\sigma_Y = max(\sigma_x^2 - \sigma_n^2, 0) \quad (8)$$

Where

$$\sigma_x^2 = \frac{1}{R^2} \sum_m^R - RC_i^2 \quad (9)$$

And R is the patch size.

Further the thresholding can be applied both as soft thresholding and hard thresholding and this approach used soft thresholding only and it is represented as

$$\hat{Y} = \begin{cases} sgn(X)(|X| - \lambda |X|^3 \lambda) \\ 0 \; |X| < \lambda \end{cases} \quad (10)$$

Where λ is the threshold value, X is the wavelet coefficients and the Y is the output value using wavelet threshold shrinkage function.

D. Fusion

The obtained denoised wavelet coefficients through two different thresholding approaches are now processed for fusion according to the correlation existing between them. Here the correlation coefficient is accomplished as a threshold to determine which wavelet coefficient was more effectively denoised [29]. Non-overlapping block correlation is measured for denoised wavelet coefficients with a patch size of 3*3. The average of all the correlation coefficients is measured further to decide the threshold value and it is denoted as T. The mathematical formula for the correlation coefficient is written as

$$CC = \frac{\sum_{i=0}^{M} \sum_{j=0}^{N} (A(i,j) - \bar{A})(B(i,j) - \bar{B})}{\sqrt{((A(i,j) - \bar{A})^2)((B(i,j) - \bar{B})^2)}} \quad (11)$$

Where

$$\bar{A} = mean(A) \quad (12)$$

$$\bar{B} = mean(B) \quad (13)$$

And the terms M and N in eq.(11) denotes the Row size and Colom sizes respectively. Here the terms Ā and represents the denoised patches of wavelet sub bands through two different thresholding mechanisms. The value of CC lies in the range of [-1, 1], where 1 specifies the strong positive correlation and -1 specifies strong negative correlation and '0' specifies no correlation. Depends on the correlation coefficient value, the two denoised patches of all wavelet sub bands are fused into one patch. Here the individual patches obtained through two different threshold mechanisms are represented as A_{M1}^k and B_{M1}^k, where M1 represents the Method 1 and M2 represents Method 2, k represents the band and its $k \in LH, HL, HH$. The correlation coefficient is evaluated between every two patches and based on the obtained CC values, the fusion is accomplished according to the following formula.

$$F_{New}^k = \begin{cases} maximum(A_{M1}^k, B_{M1}^k), If(CC \le T) \\ Average(A_{M1}^k, B_{M1}^k), If(CC > T) \end{cases} \quad (14)$$

Finally the obtained denoised patches are aggregated and over the aggregated patches, inverse DT-CWT was accomplished to reconstruct the denoisedimage.

IV. SIMULATION RESULTS

To simulate the developed denoising framework, various test images are used. The simulation is accomplished using the MATLAB software. Simulation is carried out under various types of noises with various noise levels and at every simulation; the performance evaluation is carried out both qualitatively and quantitatively. The qualitative evaluation is accomplished through visual observation and the quantitative evaluation is accomplished through the performance metrics namely, Peak Signal to Noise Ratio (PSNR), Structural Similarity Index Measure (SSIM), and Pratt's figure of merit (FOM) [46]. The test images considered for simulation are shown in figure.3.

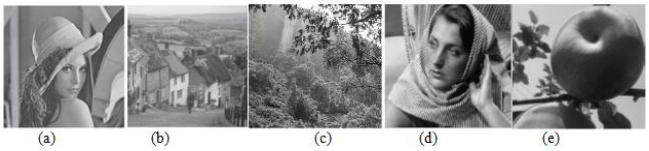

Figure.3 Test images, (a) Lena, (b) Houses, (c) Forest, (d) Barbara and (e) Apple

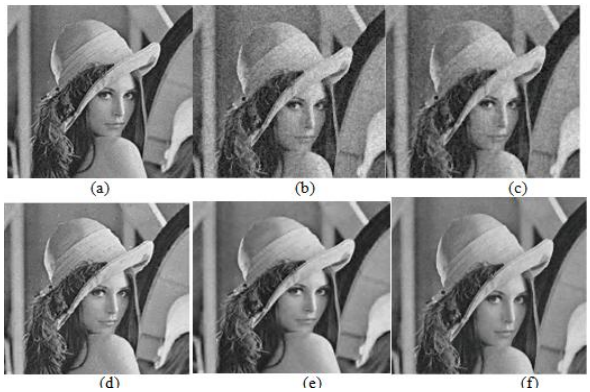

Figure.4 Results of Lena image, (a) Noisy image, denoised through (b) WT-SVD-DF, [24],(c) WT-IC [25], (d) DT-CWT-PG [38], (e) DT-CWT-GPG [45], and (f) Proposed

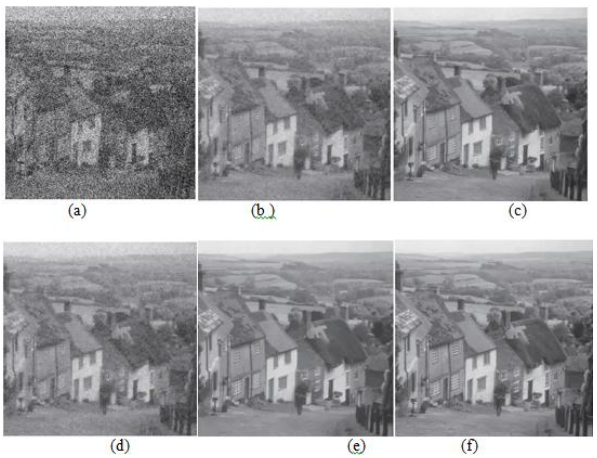

Figure.5 Results of Houses image, (a) Noisy image, Denoised through (b) WT-SVD-DF, [24], (c) WT-IC [25], (d) DT-CWT-PG [38], (e) DT-CWT-GPG [45], and (f) Proposed

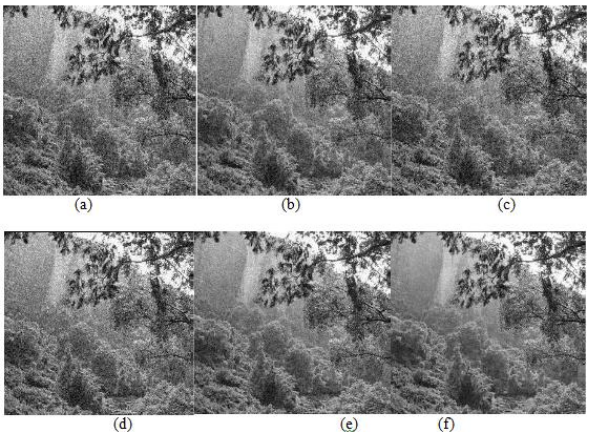

Figure.6 Results of Forest image, (a) Noisy image, Denoised through (b) WT-SVD-DF, [24], (c) WT-IC [25], (d) DT-CWT-PG [38], (e) DT-CWT-GPG [45], and (f) Proposed

Figure.7 Results of Barbara image, (a) Noisy image, Denoised through (b) WT-SVD-DF, [24], (c) WT-IC [25], (d) DT-CWT-PG [38], (e) DT-CWT-GPG [45], and (f) Proposed

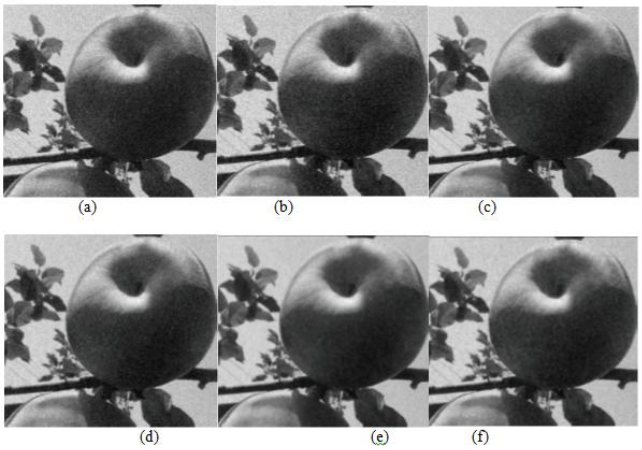

Figure.8 Results of Mountain image, (a) Noisy image, Denoised through (b) WT-SVD-DF, [24], (c) WT-IC [25], (d) DT-CWT-PG [38], (e) DT-CWT-GPG [45], and (f) Proposed

The obtained denoised image results after the accomplishment of propsoed approach over the test images are depicted in the above figures. Figure.4 depicts the results of Lena image, Figure.5 depicts Houses Image results, Figure.6 depicts the results of Forest image, Figure.7 is of Barbara image and Figure.8 shows the results of Apple image. From all the above figures, it can be noticed that the visual qaulity of the denosied image obtained through proposed approach is more qualitative and also preserved the edge features. Even in the images with dense edges (e.g. Forest), the proposed approach tried to preserve all the edge pixels with less infomration loss. In the above results, the denoise images obtained through conventional approaches, Wavelet Transform and Singular value decomposition combined with directional filter (WT-SVD-DF) [24], Wavwlet Transform considering with Intercorrelation (WT-IC), DT-CWT with patch grouping (DT-CWT-PG), and DT-CWT with gradient based Patch Grouping (DT-CWT-GPG)

are also depicted. Compared to the denosied images obtained through conventional approahces, the results of propsoed approach are more efficient.

Further to check the performance, the obtained denoised image are processed for objective evalutaion through some performance metrics like PSNR and SSIM. The mathematical formulae of PSNR and SSIM is described as follows;

$$PSNR = 10 * \log 10\left(\frac{Max^2}{MSE}\right) \qquad (15)$$

MAX is the maximum value of pixels (255 for grey scale images). MSE is the Mean Square Error between the original and denoised images. It is given by equation (16).

$$MSE = \frac{1}{mn}\sum_{i=1}^{m}\sum_{i=1}^{n}(O(i,j) - D(i,j))^2 \qquad (16)$$

O(i,j) is original image pixel and *D(i,j)* is denoised image pixel. Greater PSNR values indicate better quality. It is expressed in decibels (dB).

SSIM is an objective image quality metric and is superior to traditional measures such as MSE and PSNR. PSNR estimates the perceived errors, whereas SSIM considers image degradation as perceived change in structural information. Structural information is the idea that the pixels have strong interdependencies especially when they are spatially close. These dependencies carry important information about the structure of the objects in the visual scene. The SSIM is given by equation (17).

$$SSIM = \frac{(2 * \bar{x} * \bar{y} + c_1)(2 * \sigma_{xy} + C_2)}{(\sigma_x^2 + \sigma_y^2 + c_1)(\bar{x}^2 + \bar{y}^2 + C_2)} \qquad (17)$$

Where C1 = $(k1L)^2$, and C2 = $(k2L)^2$ are two constants used to avoid null denominator. L is the dynamic range of the pixel values. k1 = 0.01 and k2 = 0.03 by default.The dynamic range of SSIM is between -1 and 1. Maximum value of 1 will be obtained for identical images.

To measure the performance of denoising approach with respect to edge preservation, Pratt's Figure of Merit [46] is a most widely used metric. This metric illustrates the performance by checking the coincidence of original edges with the edges in the denoised image. The FOM is defined as;

$$FOM = \frac{1}{max(N_{Ide}N_{Det})}\sum_{i=1}^{N_{det}}\frac{1}{1+\alpha d_i^2} \qquad (18)$$

Where N_{Ide} and N_{Det} are the total number if Ideal/original edges and the total number of detected edges respectively. d_i is the distance between the edge pixel and the nearest ideal edge pixel and α is an arbitrary constant which used to penalize the displaced edges. The optimal range of FOM lies in between o and 1, where the value 1 denotes that the detected edges are coincided with ideal edges.

Table.1 PSNR observations for different types of noises

Image	Noise Level	Gaussian Noise			Salt & Pepper Noise			Speckle Noise		
		PSNR	SSIM	FOM	PSNR	SSIM	FOM	PSNR	SSIM	FOM
Lena	10	34.1256	0.9896	0.8562	32.3356	0.9839	0.8647	30.2317	0.9612	0.8522
	20	33.8210	0.9763	0.8533	31.4578	0.9730	0.8571	29.8571	0.9583	0.8414
	30	33.5542	0.9701	0.8496	30.25647	0.9644	0.8503	29.0231	0.9504	0.8387
	40	32.7641	0.9610	0.8368	30.0028	0.9603	0.8457	28.6612	0.9463	0.8305
	50	31.1174	0.9542	0.82634	29.8652	0.9523	0.8386	27.1457	0.9321	0.8296
Houses	10	33.2198	0.9805	0.8471	31.4298	0.9748	0.8556	29.3259	0.9521	0.8431
	20	32.9152	0.9672	0.8422	30.5520	0.9639	0.8480	28.9513	0.9492	0.8323
	30	32.6484	0.9610	0.8405	29.3506	0.9553	0.8412	28.1173	0.9413	0.8296
	40	31.8583	0.9519	0.8277	29.0970	0.9512	0.8366	27.7554	0.9372	0.8214
	50	30.2116	0.9451	0.8172	28.9594	0.9432	0.8295	26.2399	0.9230	0.8205
.Forest	10	32.2106	0.9741	0.8446	30.4206	0.9645	0.8551	28.3167	0.9517	0.8426
	20	31.9060	0.9667	0.8437	29.5428	0.9574	0.8475	27.9421	0.9423	0.8318
	30	31.6392	0.9523	0.8400	28.3414	0.9441	0.8407	27.1081	0.9323	0.8212
	40	30.8491	0.9421	0.8272	28.0878	0.9386	0.8361	26.7462	0.9237	0.8152
	50	29.2024	0.9336	0.8068	27.9502	0.9259	0.8290	25.2307	0.9209	0.8103
Barbara	10	34.2832	0.9800	0.8554	32.4932	0.9823	0.8631	30.3893	0.9596	0.8506
	20	33.9786	0.9747	0.8517	31.6154	0.9713	0.8555	30.0147	0.9567	0.8393
	30	33.7118	0.9685	0.8480	30.4140	0.9628	0.8487	29.1837	0.9488	0.8298
	40	32.9217	0.9594	0.8352	30.1604	0.9587	0.8441	28.8188	0.9347	0.8147
	50	31.2750	0.9526	0.8248	30.0228	0.9507	0.8370	27.3033	0.9325	0.8110
Apple	10	33.1684	0.9775	0.8465	31.3784	0.9742	0.8550	29.2745	0.9515	0.8425
	20	32.8638	0.9666	0.8436	30.5006	0.9633	0.8474	28.8999	0.9486	0.8317
	30	32.5970	0.9604	0.8399	29.2992	0.9547	0.8406	28.0659	0.9407	0.8290
	40	31.8069	0.9523	0.8271	29.0456	0.9506	0.8360	27.7040	0.9366	0.8208
	50	30.1602	0.9445	0.8166	28.9080	0.9426	0.8289	26.1885	0.9224	0.8186

After measuring the performance metrics such as PSNR, SSIM and FOM over the obtained denoised images through proposed approach, they are tabulated intable.1. As per the table.1, the test images were processed through three types of noises, namely, Gaussian noise, Salt & pepper noise and Speckle noise by varying the noise levels from 10 to 50. The obtained values at every test case are represented in table.1. As it can be observed from table.1, as the noise level increases, the performance of proposed approach is decreasing and the decrement can be observed through the values moving from top to bottom in every Colum at every image. For entire image set, the noise is varied and the results are obtained accordingly. Furthermore, it can also be observed that the results obtained through proposed approach are illustrating an optimal performance with respect to both noise removal and edge preservation. Here the PSNR is used to depict the performance for quality evaluation.

As the PSNR values are optimal, the quality of image is considered to be optimal. Next, the SSIM also measures the quality through the structural similarity. The higher value of SSIM declares that the original image and denoised image are structurally similar. Further to measure the performance with respect to the edge preservation, a new metric, FOM was evaluated and the obtained values are observed to be almost equal to one. As itself the FOM determines the edges comparison in the original and denoised image, the value nearer to one denotes that the denoised image had almost equal edges with original image. Moreover, the accomplishment of proposed approach is as it is in the case of image contaminated with Gaussian noise and salt & pepper noises. In the case of speckle noise, initially the noisy image is transformed through natural Log Transform to realize the multiplicative nature of speckle noise.

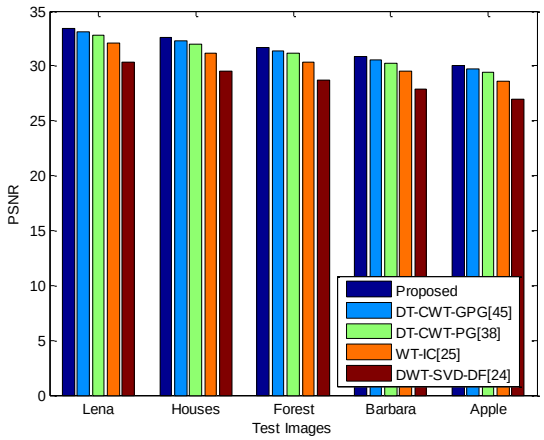

Figure.9 PSNR comparison at various noise levels for various images

The comparative analysis through PSNR, SSIM and FOM between the proposed and conventional approaches is shown in figure.9, 10 and 11 respectively. The values depicted in these figures are average values obtained over averaging the values obtained at three types of noises. From figure.9, the average PSNR of proposed approach is observed to be high compared to the conventional approaches, for all test images. Since the proposed approach accomplished both an adaptive thresholding, the PSNR value is high. The proposed approach also developed a novel patch grouping mechanism based on the Gradients of image such that the regions with similar properties are grouped into a same group. This process reduces the computational burden over the system and also increases the quality due to the accomplishment of an optimal threshold over the noisy edge. Furthermore, the proposed dual thresholding mechanism also helped in the achievement of greater quality in the denoised image by reducing the noise. Whereas, in the conventional approaches, only single thresholding technique is applied over the noisy coefficients and also not given much attention on the accurate edge detection. Similarly, the comparative analysis through the SSIM for different methods and also for different images is depicted in figure.10.

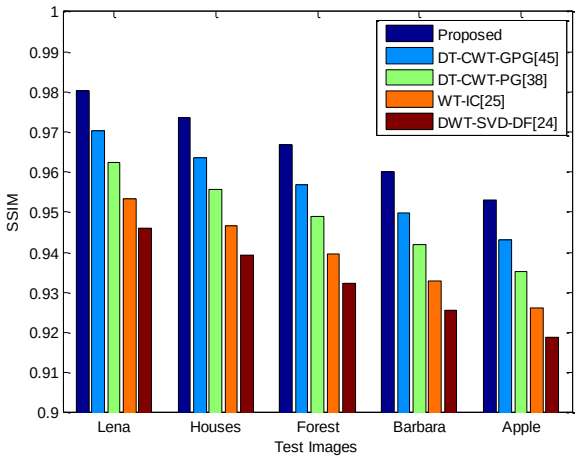

Figure.10 SSIM comparison at various noise levels for various images

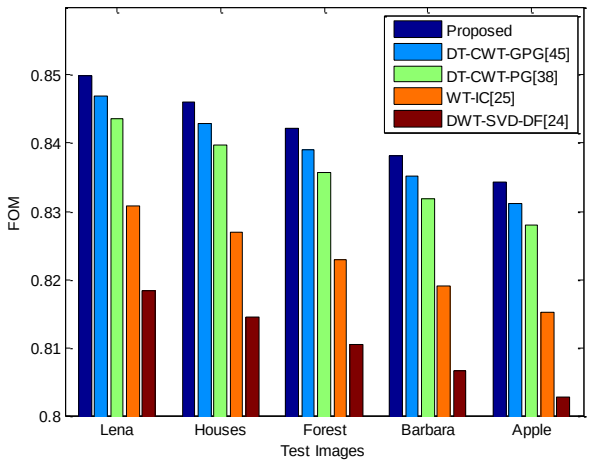

Figure.11 FOM comparison at various noise levels for various images

Figure.11 shows the comparison between the proposed and conventional approaches through the performance metrics, FOM. From figure.11, the observed FOM of proposed method is high compared to the conventional approaches. The conventional approaches, DWT-SVD-DF and WT-IC didn't focus on the edge preservation and only focused on the noise removal. The other methods such as,

DT-CWT-PG and DT-CWT-GPG focused on the edge preservation but, the overall edges are not preserved because of which the quality is less. The method proposed in [38] assumed that the noisy pixels are correlated with edge pixels and the amplitudes are almost same. To discriminate them, the energy features are considered for thresholding in the high frequency bands of noisy image. Further, the method in [45] considered Gradients of Pixels to find out the edge pixels in the image. A new feature is proposed by through which the pixels are grouped into clusters and over the patches; an energy feature oriented thresholding is applied. Though these approaches obtained better results, the false positive rate is high, i.e., the all edge pixels are not discovered and some of the noisy pixels are discovered as edges and vice versa. This constitutes an information loss and reduced the quality. Since, the proposed approach focused mostly on the edge detection the FOM is high compared to the FOM of conventional approaches.

V. CONCLUSION

This paper developed a novel image denoising framework for better edge preservation based on the Dual tree complex wavelet Transform and Gabor filter. Here the Gabor filter is mainly accomplished to find the Orientational features, i.e., in direction which is mainly the edges are concentrated. And based on the Gabor filtered edges, the regions with similar characteristics are clustered through-means algorithm. Further, a novel dual thresholding mechanism also developed in this paper to make the denoising method robust to all types of noises. Simulation experiments conducted over different test images with different noise at different noise levels revealed the performance enhancement of proposed approach. The performance is measured through the performance metrics like PSNR, SSIM and FOM and the obtained values shown an outstanding performance in the removal of noise with less information loss.

REFERENCES

1. K. Panetta, L. Bao, and S. Agaian, ``Sequence-to-sequence similarity based filter for image denoising," IEEE Sensors J., vol. 16, no. 11,pp. 4380_4388, Jun. 2016.
2. J. Liu et al., ``3D feature constrained reconstruction for low-dose CTimaging," IEEE Trans. Circuits Syst. Video Technol., vol. 28, no. 5,pp. 1232_1247, May 2018.
3. W. Zhang, B. Ma, K. Liu, and R. Huang, ``Video-based pedestrian re-identification by adaptive Spatio-temporal appearance model," IEEETrans. Image Process., vol. 26, no. 4, pp. 2042_2054, Apr. 2017.
4. Y. Chen et al., ``Artifact suppressed dictionary learning for low-doseCT image processing," IEEE Trans. Med. Imag., vol. 33, no. 12,pp. 2271_2292, Dec. 2014.
5. P. Chatterjee and P. Milanfar, ``Is denoising dead?" IEEE Trans. ImageProcess., vol. 19, no. 4, pp. 895_911, Apr. 2010.
6. A. Ben Hamza, P. Luque, J. Martinez, and R. Roman, "Removing noise and preserving details with relaxed median filters," J. Math. Imag. Vision, vol. 11, no. 2, pp. 161–177, Oct. 1999.
7. David L. Donoho and Iain M. Johnstone., "Adapting to unknown smoothness via wavelet shrinkage", Journal of the American Statistical Association, vol.90, no432, pp.1200-1224, December 1995. National Laboratory, July 27, 2001.
8. V. Strela. "Denoising via block Wiener filtering in wavelet domain". In 3rd European Congress of Mathematics, Barcelona, July 2000. Birkhäuser Verlag.
9. H. Zhang, Aria Nosratinia, and R. O. Wells, Jr., "Image denoising via wavelet-domain spatially adaptive FIR Wiener filtering", in IEEE Proc. Int. Conf. Acoust., Speech, Signal Processing, Istanbul, Turkey, June 2000.
10. Marteen Jansen, Ph. D. Thesis in "Wavelet thresholding and noise reduction" 2000.
11. M. Lang, H. Guo, J.E. Odegard, and C.S. Burrus, "Nonlinear processing of a shift invariant DWT for noise reduction," SPIE, Mathematical Imaging: Wavelet Applications for Dual Use, April 1995.
12. T. D. Bui and G. Y. Chen, "Translation-invariant denoising using multiwavelets", IEEE Transactions on Signal Processing, Vol.46, No.12, pp.3414-3420, 1998.
13. J. K. Romberg, H. Choi, and R. G. Baraniuk, "Bayesian tree-structured image modeling using wavelet-domain hidden Markov models", IEEE Image Process., Vol. 10, No 7, Jul. 2001, pp. 1056-1068.
14. J. Romberg, H. Choi and R. G. Baraniuk, "Bayesian wavelet domain image modeling using hidden Markov models," IEEE Transactions on Image Processing, vol. 10, pp. 1056-1068, July 2001.
15. A. Jung, "An introduction to a new data analysis tool: Independent Component Analysis", Proceedings of Workshop GK "Nonlinearity" - Regensburg, Oct. 2001.
16. F. Luisier, T. Blu, and M. Unser, "A new SURE approach to imagedenoising: Interscale orthonormal wavelet thresholding," IEEE Trans.Image Process., vol. 16, no. 3, pp. 593–606, Mar. 2007.
17. Q. Guo and S. Yu, "Image denoising using a multivariate shrinkagefunction in the curvelet domain," IEICE Electron. Exp., vol. 7, no. 3,pp. 126–131, Feb. 2010.
18. S. G. Chang, B. Yu, and M. Vetterli, "Adaptive wavelet thresholding forimage denoising and compression," IEEE Trans. Image Process., vol. 9,no. 9, pp. 1532–1546, Sep. 2000.
19. L. Sendur and I. W. Selesnick, "Bivariate shrinkage functions forwavelet-based denoising exploiting interscale dependency," IEEE Trans.Signal Process., vol. 50, no. 11, pp. 2744–2756, Nov. 2002.
20. A. Pižurica and W. Philips, "Estimating the probability of the presenceof a signal of interest in multi-resolution single- and multiband imagedenoising," IEEE Trans. Image Process., vol. 15, no. 3, pp. 654–665, Mar. 2006.
21. Donoho, D. L.: Denoising by Soft Thresholding. IEEE Trans. on Information Theory, 41(3), 613-627, 1995.
22. A. Fathi and A. R. Naghsh-Nilchi, "Efficient image denoisingmethod based on a new adaptive wavelet packet thresholdingfunction," IEEE Transactions on Image Processing, vol. 21, no. 9,pp. 3981–3990, 2012.
23. P. Jain andV. Tyagi, "An adaptive edge-preserving image denoisingtechnique using patch-based weighted-SVD filtering inwavelet domain,"Multimedia Tools and Applications, vol. 76,no.2, pp. 1659–1679, 2017.
24. M.Wang, Z. Li, X. Duan, andW. Li, "An image denoisingmethodwith enhancement of the directional features based onwavelet and SVD transforms," Mathematical Problems in Engineering,vol. 2015,Article ID 469350, 9 pages, 2015.
25. C.He,J.Xing, J. Li,Q. Yang, andR.Wang, "Anewwavelet thresholddeterminationmethod considering interscale correlation insignal denoising," Mathematical Problems in Engineering, vol.2015, Article ID280251, 9 pages, 2015.
26. H.-C. Li, W. Hong, Y.-R. Wu, and P.-Z. Fan, "Bayesian waveletshrinkagewith heterogeneity-adaptive threshold for SAR imagedespeckling based on generalized gamma distribution," IEEETransactions on Geoscience and Remote Sensing, vol. 51, no. 4,pp. 2388–2402, 2013.

27. M. Jansen and A. Bultheel, "Multiple wavelet threshold estimationby generalized cross validation for images with correlatednoise," IEEE Transactions on Image Processing, vol. 8, no. 7, pp.947–953, 1999.
28. Singh, Prabhishek, Shree, Raj, 2016. Analysis and effects of speckle noise in SARimages, published in 2nd International Conference on Advances in Computing,Communication, & Automation (ICACCA) (Fall) Pages: 1–5, IEEE ConferencePublications.
29. Singh, Prabhishek, Shree, Raj, 2017. Statistical Quality Analysis of Wavelet BasedSAR Images in Despeckling Process. Asian J. Electr. Sci. (AJES) 6 (2), 1–18.
30. Singh, Prabhishek, Shree, Raj, 2017. Quantitative Dual Nature Analysis of MeanSquare Error in SAR Image Despeckling. Int. J. Comput. Sci. Eng. (IJCSE) 9 (11),619–622.
31. Manoj, Kumar, Manoj, 2014. CT image noise reduction based on adaptivewiener filtering with Wavelet packet thresholding. In: Parallel, Distributed andGrid Computing (PDGC), 2014 International Conference, 11–13 Dec. 2014,doi:10.1109/PDGC.2014.7030722.
32. Kumar, Manoj, Diwakar, Manoj, 2016. New Locally Adaptive Patch Variation BasedCT Image Denoising. Int. J. Image Graph. Signal Process. (IJIGSP) 8 (1), 43–50.
33. Sethunadh, R., Thomas, T., 2014. Spatially adaptive despeckling of SAR image usingbivariate thresholding in directionlet domain. Electr. Lett. 50 (1), 44–45.
34. Ranjani, J.J., Thiruvengadam, S.J., Jun. 2010. Dual tree complex wavelet transformbased despeckling using interscale dependency. IEEE Trans. Geosci. RemoteSens. 48 (6), 2723–2731.
35. Bin, Xu, Cui, Yi, Li, Zenghui, Zuo, Bin, Yang, Jian, Song, Jianshe, 2015. Patch Ordering-Based SAR Image Despeckling Via Transform-Domain Filtering. IEEE J. SelectedTop. Appl. Earth Observ. Remote Sens. 8 (4), 1682–1695.
36. K. Dabov, A. Foi, V. Katkovnik, K. Egiazarian, Image denoising with block-matching and 3D filtering, in: SPIE Electronic Imaging: Algorithms andSystems, vol. 6064, 2006, pp. 606414-1–606414-12.
37. M. Maggioni, V. Katkovnik, K. Egiazarian, A. Foi, Nonlocal transform-domain filter for volumetric data denoising and reconstruction, IEEE Trans. ImageProcess. 22 (1) (2013) 119–133.
38. B.Chinna Rao M., Madhavi Latha, "An Image Denoising Framework Based on Patch Grouping In Complex Wavelet Domain", International Journal of Computers Communications & Control, vol.13, issue.5, 2018.
39. K. Dabov et al., "Image denoising by sparse 3-D transform-domaincollaborative filtering," IEEE Trans. Image Process. 16, 2080–2095(2007).
40. M. Elad and M. Aharon, "Image denoising via sparse and redundantrepresentations over learned dictionaries," IEEE Trans. ImageProcess. 15, 3736–3745 (2006).
41. P. Chatterjee and P. Milanfar, "Clustering-based denoising with locallylearned dictionaries," IEEE Trans. Image Process. 18, 1438–1451(2009).